GEOLOGICA CARPATHICA, OCTOBER 2007, 58, 5, 415–425

High-temperature to ultrahigh-temperature metamorphism related to multiple ultrapotassic intrusions: evidence from garnet-sillimanite-cordierite kinzigite and garnet-orthopyroxene migmatites in the eastern part of the Moldanubian Zone (Bohemian Massif)

JAROMÍR LEICHMANN[1], MILAN NOVÁK[1], DAVID BURIÁNEK[2] and DAVID BURGER[1]

[1]Institute of Geological Sciences, Masaryk University, Kotlářská 2, 611 37 Brno, Czech Republic;
leichman@sci.muni.cz; mnovak@sci.muni.cz; xburger@sci.muni.cz
[2]Czech Geological Survey, Leitnerova 2, 602 00 Brno, Czech Republic; burianek@cgu.cz

(Manuscript received March 6, 2006; accepted in revised form March 15, 2007)

Abstract: The garnet-sillimanite-cordierite kinzigite from Petrovice, Jihlava Pluton, Moldanubian Zone, Czech Republic has a hyperaluminous chemical composition. Its mineral assemblage consisting of garnet and prismatic sillimanite I, relics of cordierite, hercynite, rutile I, ilmenite and quartz, retrograde minerals — cordierite II, fibrolitic sillimanite II and Ti-rich biotite and leucocratic portions with abundant K-feldspar, quartz and plagioclase which closely matches a restite. The prograde part of the reaction history was virtually obliterated and the mineral reactions: (1) Crd + Hrc = Grt + Sil; (2) Hrc + Qtz = Grt + Sil; (3) Grt + Sil + Qtz + L = Crd + Bt; (4) Grt + L = Crd + Bt + Qtz; (5) Grt + Crd + L = Bt + Sil; (6) Crd + L = Bt + Sil + Qtz took place during cooling. The relic assemblages cordierite+hercynite and hercynite+quartz, which represent a peak of metamorphism, are stable for P ~ 0.5 GPa at T > ~ 900 °C. The *P-T* conditions determined by geothermobarometry yield: T = 900 ± 40 °C (garnet–ilmenite) and P = 0.73–0.49 GPa (spinel–garnet); concentrations of Zr in rutile I enclosed in garnet and sillimanite I yielded T = 840–970 °C. We assume, on the basis of the hyperaluminous chemistry and mineral assembly that the garnet-sillimanite-cordierite kinzigite from Petrovice is a restite, where a large portion of melt was lost from the rock. The sequence of mineral reactions, and garnet composition with low and constant Ca in the profile across the grain, indicate an isobaric cooling path. A moderate heat input from the Jihlava Pluton, manifested by garnet-orthopyroxene-cordierite migmatites developed at the direct contact of durbachites, supported by a local but large heat input of gabbro–monzogabbro associated directly with kinzigites seem probable heat sources. The chemical U-Pb ages of monazite 319 ± 24 Ma from kinzigite, 329.8 ± 9.5 Ma from garnet-orthopyroxene migmatites, and 335.8 ± 6.9 Ma from gabbros are very close to U-Pb ages of zircon 335.2 ± 0.5 Ma from durbachites (Kotková et al. 2003). They suggest a Variscan age of the HT (to UHT) metamorphism and support affiliation to the durbachite intrusions.

Key words: Moldanubian Zone, Jihlava Pluton, mineral reactions, HT metamorphism, heat source, garnet-sillimanite rock, restite.

Introduction

High-temperature metamorphism commonly associated with granitoid magmatism is a major feature of the crystalline core of the Variscan orogenic belt (O'Brien 2000, see also Montel et al. 1992; Petrakakis 1997; Kalt et al. 1999; Henk et al. 2000 and references therein). Within the Moldanubian Zone, several areas with intensive and widespread HT metamorphism were distinguished: for example, cordierite-bearing migmatites with hercynite and orthopyroxene-bearing leucosome in the Bavarian Forest, where temperatures reach up to ~770–850 °C (Kalt et al. 1999); cordierite-bearing migmatites of the Monotonous Group in the envelope of the South Bohemian Pluton, with the mineral assemblages indicating temperatures of 650–800 °C (Linner 1996; Büttner & Kruhl 1997; Deibl et al. 2003).

The garnet-sillimanite-cordierite kinzigite from Petrovice, Jihlava Pluton is characterized by a hyperaluminous bulk chemical composition and mineral assemblages with abundant garnet and prismatic sillimanite I with relics of cordierite I, hercynite, ilmenite, rutile, and common retrograde cordierite II, fibrolitic sillimanite II and Ti-rich biotite. The kinzigite represents a new example of HT to UHT metamorphism in the eastern part of the Moldanubian Zone. The rock exhibits several features, which very closely resemble those attributed to restites (see e.g. Vielzeuf & Holloway 1988; Patiño Douce & Johnston 1991; Patiño Douce & McCarthy 1998). It is very similar to Al-rich rock with garnet, sillimanite, hercynite, cordierite and corundum from Sepekov near Milevsko, Central Bohemia (Fiala & Losert 1976). The hyperaluminous composition of the rock is fairly distinct from the HT cordierite-bearing migmatites mentioned above and from garnet-orthopyroxene migmatites in direct contact with the durbachite. We present mineralogical and petrological data, discuss the formation, the *P-T* conditions and evolutions of the garnet-sillimanite-cordierite kinzigite and garnet-orthopyroxene-cordierite migmatites.

Geological setting

The Moldanubian Zone represents a crustal stack of allochthonous units assembled during the Variscan orogeny. It was formed by several Variscan events of superimposed deformation phases and metamorphic recrystallizations (Dallmeyer et al. 1995; Franke 2000). Three fundamentally different tectonometamorphic units can be recognized: (i) LP/HT series; (ii) HP/L-MT series; (iii) remnants of HP/HT series (O'Brien 2000). The rocks characterized by LP/HT are commonly associated with the Variscan plutons (Novák & Houzar 1996; Linner 1996; Büttner & Kruhl 1997; Henk et al. 2000).

The Jihlava Pluton is located in the eastern part of the Moldanubian Zone, E of the South Bohemian Pluton (Fig. 1). It is mainly composed of ultrapotassic pyroxene-biotite syenites to quartz monzonites (durbachites) hosted in biotite to biotite-sillimanite ± cordierite gneisses locally strongly migmatized at the contact. Enclaves of biotite-sillimanite gneisses also form an approximately N–S trending discontinuous belt, several km long, located in the center of the Jihlava Pluton (Fig. 1). A NNW–SSE oriented body of shoshonitic to ultrapotassic gabbro to monzogabbro (Leichmann & Švancara 2005), approximately 2 km long, is situated E of the gneiss belt within the Jihlava Pluton. Monzogabbro exhibits complicated textural relations; the primary assemblage is characterized by clinopyroxene+orthopyroxene+K-feldspar+plagioclase, whereas biotite, quartz and amphibole represent secondary phases. Monzogabbro resembles mafic charnockites and a temperature of magmatic crystallization (~1000–1100 °C; Leichmann et al. 2000) was calculated from the composition of mesoperthitic K-feldspar (see Nekvasil 1992). The durbachites (syenite to quartz monzonite) from the Jihlava Pluton differ from gabbro to monzogabbro by their lower amount of mafic components and higher content of K-feldspar; nevertheless, they exhibit similar textures such as mesoperthitic K-feldspar and exsolutions of orthopyroxene in clinopyroxene. These indicate their magmatic crystallization at high temperature (T ~ 850 °C) but lower relative to the gabbro–monzogabbro.

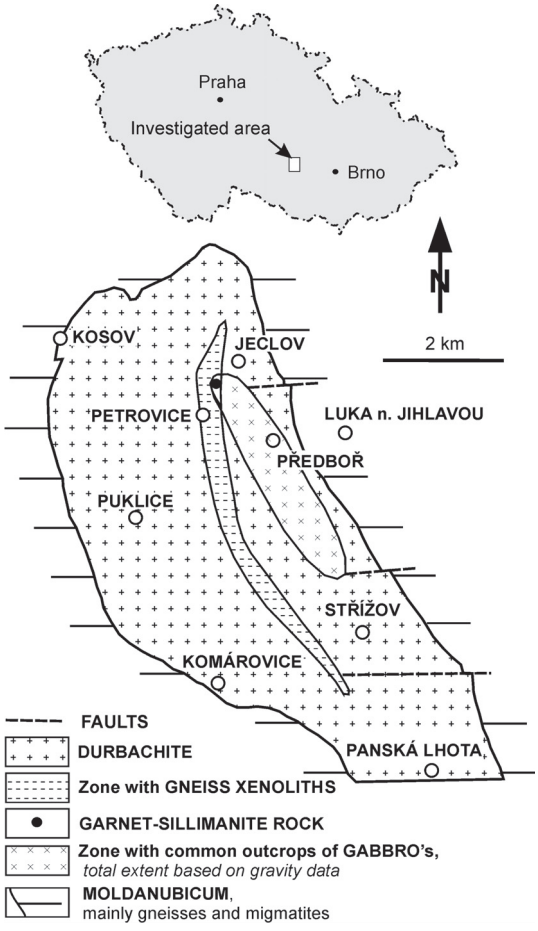

Fig. 1. Schematic geological map of the northern part of the Jihlava Pluton (modified from Tonika 1970).

Two distinct types of rocks showing HT metamorphic conditions were found within the Jihlava Pluton. The garnet-sillimanite-cordierite kinzigite forms an isolated outcrop about 15×10 m in size located at the contact between shoshonitic gabbros and gneiss. Both gabbro as well as gneiss enclave are hosted in the cpx-opx-bearing syenites to monzonites. The second type — garnet-orthopyroxene migmatite, occurring locally at the contact of Jihlava Pluton and surrounding metasedimentary rocks, forms small layers up to several dm thick. It differs from the kinzigite examined by small size, low amount of melt, less aluminous composition and simple mineral assemblage.

Analytical methods

The electron-microprobe analyses were done on a Cameca SX-100 instrument in the wavelength-dispersion mode at the Slovak Geological Survey in Bratislava. Accelerating potential was 15 kV for all elements, spot diameter 1 μm, beam current 20 nA. The samples were analysed using the $K\alpha$ lines from the following standards: albite (Na), wollastonite (Ca, Si), orthoclase (K), MgO (Mg), Fe_2O_3 (Fe), chromite (Cr), gahnite (Zn), metal Mn (Mn), Al_2O_3 (Al), TiO_2 (Ti), NaCl (Cl), BaF_2 (F). Data were reduced on-line using the PAP routine (Pouchou & Pichoir 1985). The same equipment was used for the chemical dating of monazite by the method of Montel (1996). The current of 250 nA and voltage of 15 kV were used for the determination of Th, U and Pb contents. The error of determination ranged between 0.04–0.05 wt. % for Th, 0.025–0.030 wt. % for U and about 0.01 wt. % for Pb. Monazite samples with known concordant U-Pb ages determined by classical radiogenic methods were used as standards.

Zirconium in rutile was determined on a Cameca SX-100 instrument in the wavelength-dispersion mode at the Joint Laboratory of Electron Microscopy and Microanalysis, Institute of Geological Sciences, Masaryk University, Brno and Czech Geological Survey, Prague. The accelerating voltage was 15 kV, spot diameter 1 μm, beam current 20 nA and counting time 300 s, the standard used was $ZrSiO_4$.

Part of the electron microprobe analysis was carried out on the JEOL Superprobe JXA-8600 instrument in the

wavelength-dispersion mode at the Paris Lodron University, Salzburg, Austria with beam diameter of 3 μm, accelerating voltage of 15 kV, and sample current of 20 nA. Natural minerals and oxides (Si, Al, Ti, Cr, Fe, Mn, Mg, Ba) were used as standards. Data were reduced using the ZAF-4 corrections.

Whole-rock chemical analyses were performed at the Acme Chemical Laboratories Ltd, Vancouver, by ICP-ES (main elements) and ICP-MS (trace elements and REE). The melanosome-dominant portion contains a small admixture of leucosome (about 10 %), but the leucosome portion contains modest admixture of melanosome (about 20 vol. %). We were not able to subtract the admixture of melanosome (or leucosome) completely.

Results

Macroscopic description

The garnet-sillimanite-cordierite kinzigite is heterogeneous on a macroscopic scale with volumetrically dominant melanosome consisting of coarse- to medium-grained garnet + sillimanite + cordierite + biotite. The melanosome-bearing rocks consist of approximately 50 % garnet, up to 20 % sillimanite and cordierite, while biotite forms together 30 %. It does not exhibit any apparent preferred orientation of minerals. Abundant silvery white prismatic crystals of sillimanite I, up to 1 cm long, are randomly distributed. The melanosome locally contains minor, irregularly distributed, medium-grained to locally fine-grained quartz-feldspar portions of leucosome as nets and veins, up to 3 cm in size. Leucosome could form up to 30 % of the rock. The content of retrograde cordierite and biotite increases at the expense of garnet with increasing leucosome portion. It forms a matrix, which locally surrounds early-formed minerals. Contacts between melanosome and leucosome are commonly marked by more abundant cordierite, biotite and fibrous sillimanite, sharp contacts of leucosome with sillimanite + garnet dominant rock are rare. Garnet-orthopyroxene migmatites are distinctly banded rocks, where biotite-plagioclase bands distinctly prevail over quartz-feldspar leuocosome. Small grains of garnet are randomly distributed mainly in the leucosome portion.

Petrography

The garnet-sillimanite-cordierite kinzigite displays mineral assemblages with complex textural relationships in thin sections. Melanosome consists of euhedral, prismatic crystals of sillimanite I (Fig. 2a,b), with locally abundant inclusions of cordierite I, hercynite, quartz, ilmenite and short prismatic grains of rutile I (all inclusions up to 50 μm in size) randomly distributed within crystals (Fig. 2a,b). Hercynite and quartz were not found in direct contact, they are always separated by sillimanite, but the distance of both minerals is commonly smaller than the size of their grains. Hercynite and ilmenite are commonly closely associated (Fig. 2d). Euhedral prismatic sillimanite I is weakly affected by subsequent mineral reactions (Fig. 2a,b). Anhedral to locally subhedral zoned grains of garnet, up to 5 mm in diameter, contain inclusions of cordierite I, hercynite, ilmenite, quartz and rutile I concentrated apparently in cores of garnet (Fig. 2a); abundance, volume ratios and textural relations of the individual inclusions in garnet cores are similar to those described in prismatic sillimanite I. Small inclusions of hercynite were scarcely found in cordierite I (Fig. 2d). Rare inclusions of monazite occur in garnet closely associated with other inclusions — hercynite, rutile I, cordierite I, ilmenite and quartz. Monazite is homogeneous in transmitted light as well as in the BSE image. Very rare accicular rutile II occurs in the outer parts of garnet grains, where the inclusions of cordierite I, hercynite, quartz, rutile I and ilmenite are not present. Garnet was partly consumed during mineral reactions and replaced by cordierite II ± biotite chiefly along garnet rims (Fig. 2c). Garnet cores with common inclusions were locally replaced as well, but inclusions of hercynite locally survived, whereas rutile I, cordierite I and quartz were completely consumed. Ilmenite is abundant as inclusions in early garnet and sillimanite, in cordierite II as well as in biotite I and II. It occurs very likely in several distinct types, which we were not able to distinguish. Anhedral cordierite II replacing garnet is commonly replaced by aggregate of biotite + fibrolitic sillimanite II. It seems that biotite is present in several textural and paragenetic types (Fig. 2a,b,c). Abundant coarse flakes of biotite I are commonly associated with cordierite II and/or fibrolitic sillimanite II. Small anhedral to subhedral flakes of biotite II fill late fractures in garnet (Fig. 2a). Cordierite II, biotite I and fibrolitic sillimanite II are commonly developed between aggregates of prismatic sillimanite I + garnet, and quartz-feldspar rich leucosome. Additional accessory minerals include zircon, xenotime and pyrite. During the late retrograde stage, chlorite-dominated, fine-grained pseudomorphs after cordierite II were formed (Fig. 2b,c). Orthopyroxene, kyanite and other relevant minerals (e.g. osumilite, corundum, sapphirine) were not identified.

The leucosome portions form irregular masses, veins and veinlets consisting of anhedral quartz, K-feldspar and commonly less abundant subhedral plagioclase. Both feldspars are rather homogeneous. Based on the CL and EMP study, one compositional type of K-feldspar and plagioclase, respectively, were observed. Anhedral grains of quartz associated with subhedral plagioclase occur in relatively fine-grained matrix located around large grains of sillimanite I, garnet, cordierite II and biotite.

The garnet-orthopyroxene migmatite from the exocontact of the Jihlava Pluton is composed mainly of quartz, plagioclase and biotite I. Orthopyroxene forms subhedral colourless grains, up to 1 mm in size, garnet was found as very irregular poikiloblastic grains, about 0.5 mm in diameter, with abundant inclusions of quartz. Garnet and orthopyroxene are closely spatially associated and are commonly replaced by flakes of biotite II. Irregular grains of cordierite, about 1 mm in size, commonly oc-

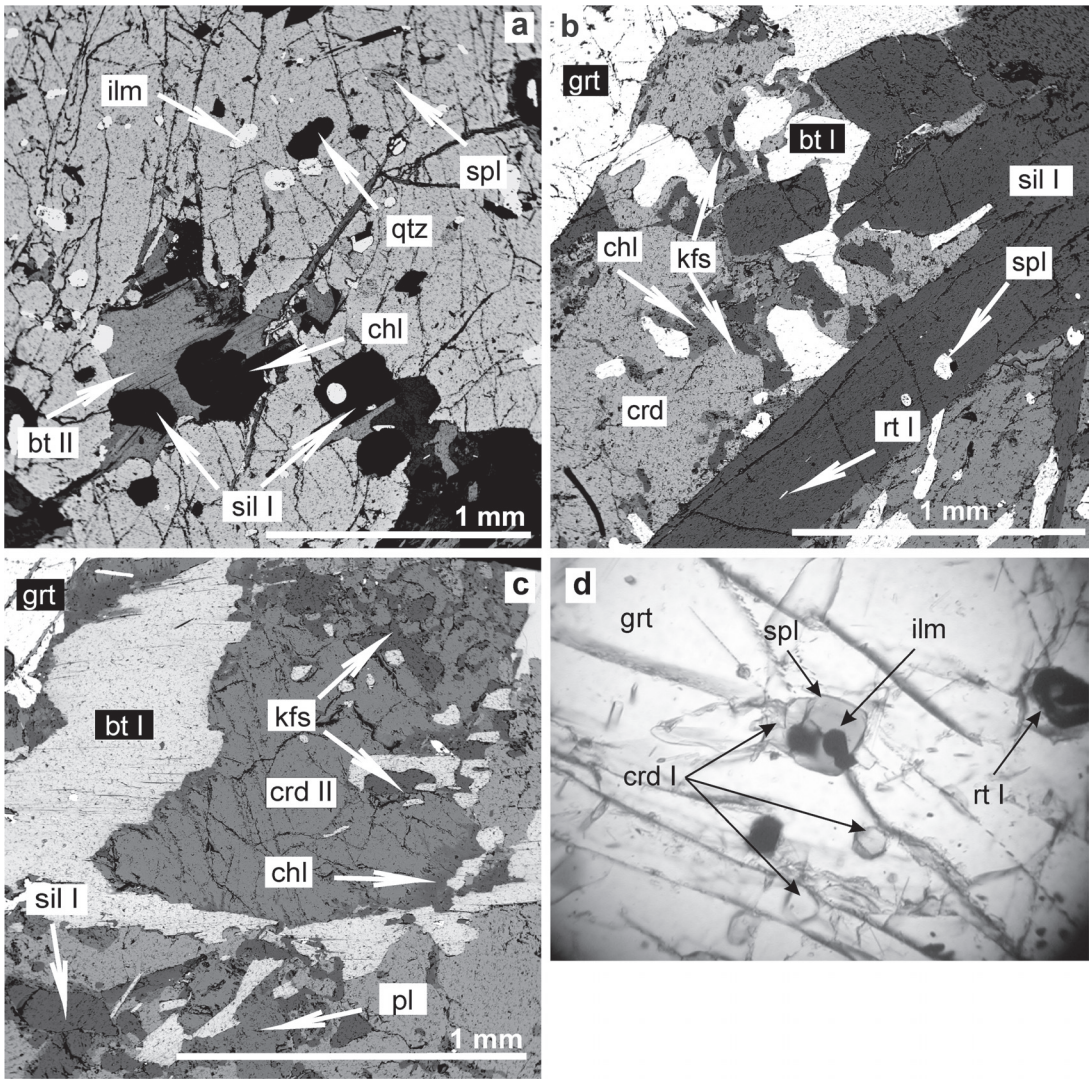

Fig. 2. BSE images of garnet-sillimanite rock. **a** — garnet with inclusions of spinel, ilmenite, and quartz, note euhedral sillimanite I and biotite II in fractures of garnet; **b** — euhedral crystals of prismatic sillimanite I with inclusions of spinel and rutile I enclosed in aggregate of cordierite + biotite I; **c** — cordierite rimmed by biotite I, note intergrowths of cordierite and K-feldspar. Abbreviations of minerals from Kretz (1983). **d** — PPL image — garnet with inclusions of spinel, cordierite I, rutile I and ilmenite.

curring in the outer part of the contact locally replaces garnet and both minerals are commonly replaced by fibrolitic sillimanite and biotite II. The assemblage garnet + orthopyroxene is mostly located close to the contact with the pluton, whereas the assemblage cordierite + sillimanite occur in a distal part.

Whole-rock chemistry

Whole-rock analyses of kinzigite yielded different results for the melanosome and for the leucosome portion (see Table 1). The melanosome exhibits hyperaluminous composition (Al_2O_3 ~ 30 wt. %, A.S.I. 8.17) and high contents of

Table 1: Representative chemical composition of garnet-sillimanite rock.

	SiO_2	Al_2O_3	Fe_2O_3	MgO	CaO	Na_2O	K_2O	TiO_2	P_2O_5	MnO	Cr_2O_3	Ba	LOI	Tot
GS	41.63	30.02	16.67	5.40	0.95	0.51	1.00	1.88	0.03	0.60	0.036	338	0.8	99.88
QF	54.24	23.63	11.88	3.58	0.82	0.72	2.05	1.28	0.01	0.045	0.29	1234	0.8	99.66
	Co	**Cs**	**Ga**	**Hf**	**Nb**	**Rb**	**Sr**	**Ta**	**Th**	**U**	**V**	**Zr**	**Y**	**Tl**
GS	43.4	14.1	39.5	8.3	32.9	65.8	83.5	2.5	6.3	3.8	253	305.8	100.4	0.4
QF	32.8	8.7	31.6	5.8	16.9	80.8	180.6	1.4	8.4	1.8	185	220.5	50.6	0.5
	La	**Ce**	**Pr**	**Nd**	**Sm**	**Eu**	**Gd**	**Tb**	**Dy**	**Ho**	**Er**	**Tm**	**Yb**	**Lu**
GS	13	25.7	2.69	12.8	5.9	1.05	11.94	2.62	17.08	3.55	11.38	1.64	10.78	1.55
QF	21.7	37.8	3.58	15.6	5	2.6	8.32	1.53	9.22	1.76	5.41	0.77	5.32	0.7

GS — garnet-sillimanite rock, **QF** — parts of the garnet-sillimanite rock, enriched on feldspars and quartz, **LOI** — loss of ignition.

Fe_2O_3tot and MgO, whereas SiO_2, CaO, Na_2O, K_2O, Ba, Sr and Rb are low. The domains consisting of dominant leucosome are characterized by elevated amounts of K_2O, SiO_2, Ba, Rb and Sr. Concentrations of HFSE are generally high, but the melanosome is systematically enriched relatively to the leucosome (Table 1). The leucosome (A.S.I. 4.71) is slightly enriched in light REE's (Eu/Eu* = 1.33; LREE 83.7 ppm, HREE 33.0 ppm) and exhibits a weak positive Eu anomaly relative to the melanosome, which is enriched in HREE's (LREE 60.1 ppm, HREE 60.5 ppm) and shows distinct negative Eu anomaly (Eu/Eu* = 2.7).

Chemical composition of minerals

Hercynite is a hercynite-spinel-gahnite solid solution (Table 2). Most inclusions exhibit similar composition

Table 2a: Representative chemical composition of minerals.

	Garnet			Cordierite			Spinel		Opx
Sample No.	**K-core**	**K-rim**	**M**	**K crd 2**	**K crd 1**	**M**	**K**	**K**	**M**
SiO_2	38.30	37.20	37.52	48.60	49.24	49.52	0.023	0.02	50.19
TiO_2	0.18	0.08	0.03	0.00	0.04	0.004	0.031	0.04	0.08
Al_2O_3	21.90	21.20	21.34	32.70	33.31	32.38	56.511	57.76	2.18
Cr_2O_3	0.00	0.00	0.00	0.00	0.00	0.00	1.463	0.77	0.04
FeO	30.80	33.90	32.97	7.30	5.52	6.94	20.619	32.70	31.23
MnO	1.66	3.40	0.88	0.13	0.11	0.11	0.078	0.17	0.18
MgO	7.39	3.86	5.27	8.95	10.65	9.16	4.423	6.07	15.96
CaO	1.26	1.23	1.64	0.00	0.04	0.05	0.00	0.00	0.26
Na_2O	0.00	0.00	0.07	0.10	0.24	0.10	0.00	0.00	0.07
ZnO	0.00	0.00	0.00	0.00	0.00	0.00	16.307	1.226	0.00
Total	101.49	100.87	99.72	97.78	99.15	98.27	99.46	98.75	100.19
Si	2.96	2.97	2.98	5.01	4.97	5.07	–	–	1.943
Ti	0.01	0.05	0.002	–	0.003	–	0.001	0.001	0.002
Al	2.00	2.00	2.00	3.97	3.96	3.90	1.935	1.937	0.100
Cr	–	–	–	–	–	–	0.033	0.017	0.001
Fe^{2+}	1.99	2.26	2.19	0.63	0.46	0.59	0.500	0.728	1.010
Mn	0.11	0.23	0.06	0.01	0.009	0.01	0.002	0.004	0.006
Mg	0.85	0.46	0.63	1.38	1.60	1.40	0.192	0.258	0.921
Ca	0.104	0.11	0.14	–	0.004	0.005	–	–	0.011
Na	–	–	0.02	0.02	0.05	0.02	–	–	0.005
Zn	–	–	–	–	–	–	0.349	0.025	–
O	12.00	12.00	12.00	18.00	18.00	18.00	4.000	4.000	6.000
SCat	8.03	8.03	8.02	11.02	11.06	10.99	3.013	2.971	4.000

K — analysis from kinzigite, **M** — analysis from garnet-orthopyroxene migmatite.

Table 2b: Representative chemical composition of minerals.

	Biotite			Feldspar				Ilmenite	
Sample No.	**K**	**K**	**M**	**K**	**K**	**K**	**M**	**K**	**K**
SiO_2	34.50	34.90	36.13	57.60	58.60	63.60	64.07	0.00	0.00
TiO_2	4.70	3.59	3.33	0.00	0.00	0.00	0.00	52.90	52.00
Al_2O_3	17.50	16.60	17.64	26.00	26.10	19.10	18.47	0.00	0.00
FeO	18.60	21.00	17.37	0.00	0.08	0.00	0.01	45.90	45.50
MnO	0.07	0.07	0.07	0.00	0.00	0.00	0.00	1.15	0.56
MgO	8.94	9.40	11.10	0.00	0.00	0.00	0.00	0.17	0.87
CaO	0.00	0.00	0.00	7.69	7.40	0.00	0.07	0.00	0.00
BaO	0.41	0.39	0.00	0.00	0.00	1.53	0.55	0.00	0.00
Na_2O	0.10	0.08	0.12	6.80	7.30	1.78	1.57	0.00	0.00
K_2O	9.26	8.75	9.82	0.28	0.15	13.60	14.04	0.00	0.00
H_2O*	3.86	3.87	3.98	0.00	0.00	0.00	0.00	0.00	0.00
Total	97.98	98.36	99.56	98.37	99.63	99.61	98.78	100.43	99.25
Si	2.67	2.70	2.72	2.62	2.63	2.96	2.991	–	–
Ti	0.27	0.21	0.19	–	–	–	–	1.00	0.99
Al	1.60	1.52	1.57	1.39	1.38	1.05	1.016	–	–
Fe^{2+}	1.20	1.36	1.09	–	0.01	–	0.000	0.96	0.97
Mn	0.01	0.01	0.01	–	–	–	–	0.02	0.01
Mg	1.03	1.09	1.25	–	–	–	–	0.01	0.01
Ca	–	–	–	0.37	0.36	–	0.004	–	–
Ba	0.01	0.00	–	–	–	–	–	–	–
Na	0.02	0.01	0.02	0.60	0.63	0.16	0.142	–	–
K	0.91	0.87	0.94	0.02	0.01	0.81	0.836	–	–
OH	1.99	2.00	2.00	–	–	–	–	–	–
O	10.00	10.00	10.00	8.00	8.00	8.00	8.000	3.00	3.00
SCat	7.72	7.76	7.79	5.00	5.00	5.00	4.989	2.00	2.00

K — analysis from kinzigite, **M** — analysis from garnet-orthopyroxene migmatite.

$Hc_{52-66}Spl_{26-37}Gah_{10-18}$, with a good negative correlation Fe/Zn and low $Cr_2O_3 < 1.46$ wt. % in all samples. Exceptionally Zn-rich (16.31 wt. % ZnO) and Zn-poor (1.23 wt. % ZnO) compositions not involved in the above formula were found. Hercynite associated with cordierite I has the composition $Hc_{55}Spl_{35}Gah_{11}$.

Garnet from kinzigite (X_{Mg}=0.30–0.16) exhibits simple zoning, with core slightly enriched in pyrope component, and rim enriched in almandine and spessartine components, whereas concentrations of Ca are low and almost constant across the grains (core — $Alm_{64}Pyr_{30}Sps_3Grs_3$, rim — $Alm_{74}Pyr_{16}Sps_6Grs_4$). A typical profile of a garnet grain is given in Fig. 3. The chemical compositions of garnet from garnet-orthopyroxene-cordierite migmatite (X_{Mg}=0.28–0.22) locally exhibits higher Ca (Grs_{4-13}).

Cordierite yielded two distinct compositions; inclusions of slightly heterogeneous cordierite I show X_{Mg}=0.73–0.79, whereas homogeneous large grains of cordierite II have X_{Mg}=0.68–0.69. Both exhibit low Na_2O contents mostly below 0.10 wt. %.

Biotite is an annite-phlogopite solid solution with substantial amount of eastonite-siderophylite components. In kinzigite, biotite I is Ti-rich with 4.48–5.51 wt. % of TiO_2 (0.26–0.31 apfu) and characterized by X_{Mg}=0.47–0.44, Si=2.65–2.67 apfu, ^{Y}Al=0.51–0.54 apfu. Biotite II has X_{Mg}=0.44, Si=2.70 and it is slightly Al- (^{Y}Al=0.43 apfu) and Ti-depleted (up to 3.59 wt. % TiO_2–0.21 apfu Ti). Low concentrations of Na and Ba of ~0.02–0.01 apfu and F<0.15 apfu are typical. Biotite from migmatite is Mg-enriched (X_{Mg}=0.61–0.55), shows slightly lower TiO_2 (3.33–4.85 wt. %), ^{Y}Al=0.38–0.22 apfu but higher Si=2.70–2.73 apfu.

Orthopyroxene from migmatite (X_{Mg}=0.49–0.48, Table 2) contains a low amount of Al_2O_3 (up to 2.18 wt. % — 0.10 apfu Al). Prismatic sillimanite I and fibrolitic sillimanite II from kinzigite are close to the end-member composition Al_2SiO_5 with low concentration of Fe_2O_3 and MgO. Plagioclase An_{39-36} from the leucosome is rather homogeneous. K-feldspar is slightly Ba-enriched, with up to 1.5 wt. % of BaO. K-feldspar from migmatites is Ba depleted (BaO 0.55 wt. %). Ilmenite has X_{Mg}=0.01–0.03 and low concentrations of Mn. Representative compositions of minerals are given in Table 2. The concentrations of Zr in rutile I inclusions, enclosed in garnet cores or in prismatic sillimanite I, vary from 750 to 2200 ppm (see Fig. 4). Monazite enclosed in garnet from kinzigite yielded a chemical age of 319±24 Ma, while monazite from migmatites has an age of 329.8±9.5 Ma.

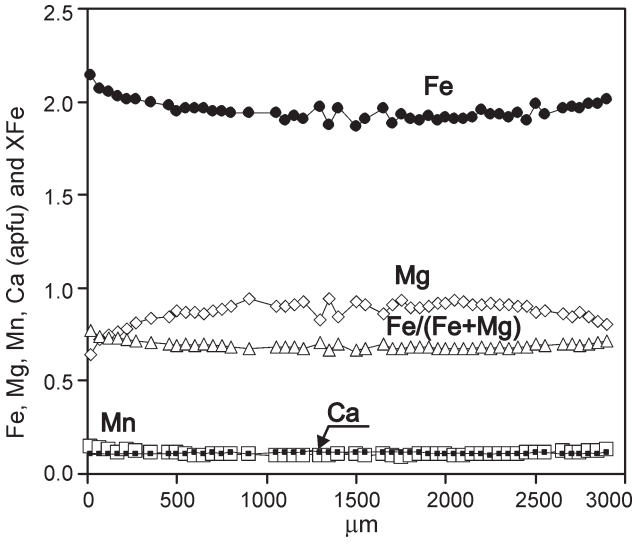

Fig. 3. A typical compositional profile of a garnet grain.

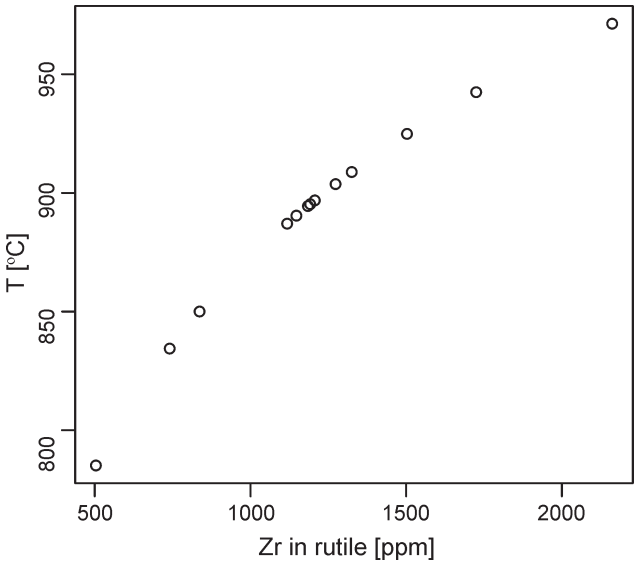

Fig. 4. Concentrations of Zr in inclusions of rutile I in garnet and sillimanite I.

Discussion

Mineral reactions and petrogenetic grid

The metamorphic evolution of garnet-sillimanite-cordierite kinzigite is illustrated in a petrogenetic grid in the KFMASH system and its derivates. Abundant ilmenite and rutile I inclusions and high Ti in biotite indicate substantial participation of TiO_2 as a minor extra component in the system.

The early mineral assemblage *A* (Table 3) is defined by abundant inclusions of cordierite I + hercynite + ilmenite + + rutile I + quartz enclosed in prismatic sillimanite I and in cores of garnet (Fig. 2a,c). Textural relations strongly suggest that this mineral assemblage represents the earliest stage recorded in the garnet-sillimanite-cordierite kinzigite. The reactions producing cordierite I, hercynite, ilmenite, rutile I, and quartz cannot be constrained due to absence of early-formed minerals. The occurrence of a relatively abundant assemblage of ilmenite + rutile + hercynite indicates breakdown of a Ti-rich spinel mineral such as ulvöspinel (see Sengupta et al. 1999); however, the textural relations are not developed enough to specify the reaction.

The mineral assemblage *B*, volumetrically dominant in the melanosome, is characterized by prismatic sillimanite I +

+garnet and represents the second stage of the evolution. Relics of cordierite I plus hercynite (in direct contact) found in garnet cores suggest that the mineral assemblage *B* formed via the FMAS reaction (Fig. 5):

$$Crd + Hrc = Grt + Sil. \quad (1)$$

Relics of hercynite and quartz (not in direct contact) occurring in sillimanite I and in garnet cores may suggest the reaction:

$$Hrc + Qtz = Grt + Sil. \quad (2)$$

The presence of melts during the reactions (1) and (2) is unclear, but formation of the assemblage garnet+sillimanite and garnet alone may have proceeded via more complicated reactions in the KFMASH system. High Zn contents in some hercynite may come from early staurolite.

The mineral assemblage *C*, characterized by the assemblage cordierite II ± biotite (Fig. 2b,c, Fig. 6, Table 3), represents the third stage. The reactions (3) and (4) are portrayed in the relevant KFMASH system:

$$Grt + Sil + Qtz + L = Crd + Bt, \quad (3)$$

$$Grt + L = Crd + Bt + Qtz. \quad (4)$$

Table 3: Mineral assemblages A–D.

Mineral assemblage	Composition
A	Crd I, Sp, Ilm, Rt, Qtz
B	Grt, Sil I
C	Crd II, Bt
D	Bt I+II, Sil II

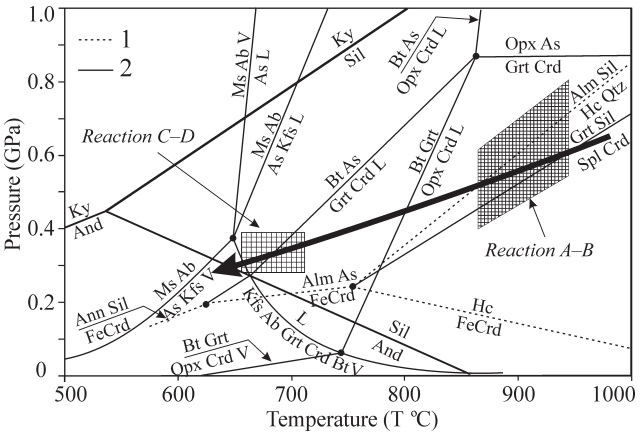

Fig. 5. *P-T* diagram for the KFMASH system showing the locations of selected melting and dehydratation reactions (modified from Spear et al. 1999). Dashed field (reaction A–B) calculated from garnet-ilmenite thermometer (Powneeby et al. 1991) and spinel-garnet geobarometer (Nichols et al. 1992). The arrow indicates the path of cooling. The $X_{Mg} = 0.33$ in hercynite relative to $X_{Mg} = 0.30$ in associated garnet shifts position of the reaction Alm + Sill = Hc + Qtz to the higher-pressure side of the reaction Alm + Sill = Spl + Crd (Spear et al. 1999 — see Fig. 3).

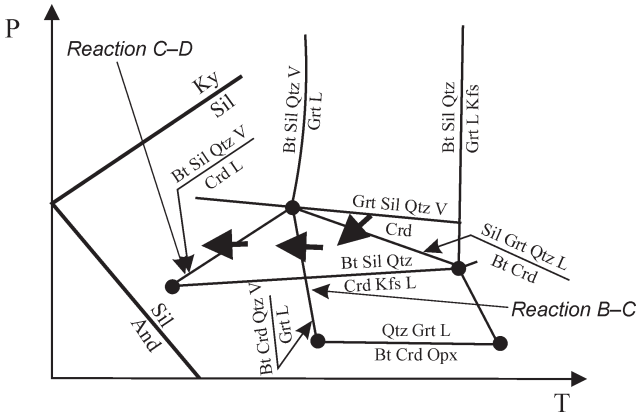

Fig. 6. Schematic *P-T* diagram for KFMASH system showing selected reactions involving cordierite (modified from Vielzeuf & Holloway 1988). The arrows mark reaction directions in the garnet-sillimanite rock.

They include garnet, sillimanite, quartz and melt as reactants; however, the textural relations show that prismatic sillimanite I is rather stable during these reactions (Fig. 2b). It may suggest significant participation of the reaction (4) relative to the reaction (3). Rare hercynite inclusions in cordierite II show that it was not or it was only partly consumed during garnet decomposition. Rutile I was likely consumed during the above reactions and Ti was incorporated into Ti-rich biotite and/or ilmenite. Ilmenite inclusions are common in both cordierite II and garnet, thus ilmenite did not participate in the reactions or it was more likely newly formed along with cordierite II, biotite and K-feldspar.

The volumetrically abundant mineral assemblage ***D*** involving biotite+fibrolitic sillimanite II is produced at the expense of garnet and particularly cordierite II via the reactions (Figs. 5, 6):

$$Grt + Crd + L = Bt + Sil, \quad (5)$$

$$Crd + L = Bt + Sil + Qtz. \quad (6)$$

As in the reactions (3) and (4), the presence of melt is required in the reactions (5) and (6). Abundance of the mineral assemblages ***C*** and ***D*** suggests essential participation of melt in the back (cooling) reactions.

Absence of orthopyroxene is a typical feature of garnet-sillimanite-cordierite kinzigite from Petrovice disregarding the fact that the estimated *P-T* conditions are suitable to produce this mineral. The hyperaluminous nature of the rock seems to be a crucial factor, which controls the absence of orthopyroxene. We assume that all Fe+Mg were consumed by garnet and the remaining Si and Al were accommodated in sillimanite.

Textural relations in garnet-orthopyroxene-cordierite migmatite are also complicated. Orthopyroxene probably originated by melting of biotite by the reaction:

$$Bt + Pl + Qtz = Opx + Kfs + L + Grt \quad (7)$$

(see Vielzeuf & Montel 1994). Other textural relations indicate a similar cooling path as in the kinzigites as documented by the reactions (4), (5) and (6) However, no relics of spinel, rutile, ilmenite or Mg-rich cordierite, common in the garnet and sillimanite I from kinzigite, were found, hence the prograde evolution of both rocks was probably different. The position of garnet in leucosome indicates that the garnet represents a restite phase remaining after melt producing breakdown of biotite I.

Estimation of metamorphic conditions

Kinzigite

The mineral assemblages, textural relations and chemical composition of minerals indicate a complex metamorphic evolution of the garnet-sillimanite-cordierite kinzigite. The diagnostic mineral assemblages and mineral reactions define the individual metamorphic stages ***A*** to ***D***. However, the resetting of the assemblages during cooling, documented by the retrograde zoning of the garnet, exclude the application of most Fe-Mg cation-exchange thermometers for the estimation of the peak metamorphic conditions. The high disequilibrium in mineral assemblages, presence of melt in the reactions followed by widespread back reactions, and absence of orthopyroxene and plagioclase in the metamorphic mineral assemblages A+B excludes the application of multielement geothermobarometers, like GASP (garnet-alumosilicate-plagioclase) or GRAIL (garnet-rutile-alumosilicate-ilmenite). The assemblage ***A*** represented by the assemblage cordierite I+hercynite+rutile I+ilmenite+quartz may record peak conditions in garnet-sillimanite-cordierite kinzigite. We have several lines of evidence, which suggest HT to perhaps UHT metamorphic conditions:

a) The assemblage cordierite I+hercynite is stable in the LP/HT field in the *P-T* diagram (see Fig. 5); high X_{Mg}=0.73–0.79 in cordierite I suggests high temperature at T>~900 °C at P~0.5–0.7 GPa (see Fig. 5).

b) The assemblage hercynite+quartz shows a similar stability field (Fig. 5), but high concentrations of Zn in hercynite indicate higher pressure (Shulters & Bohlen 1989; Dasgupta et al. 1995) and elevated spinel component in hercynite supports higher temperature (Waters 1991) relative to the end-member hercynite. Nevertheless, hercynite and quartz, although closely associated, were not found in direct contact, so this evidence is not sufficient for UHT conditions. Moreover, we do not know the parental mineral reaction producing hercynite. It may have formed by breakdown of sillimanite, kyanite and/or staurolite (Spear et al. 1999), which may be a source of Zn in hercynite. Nevertheless, crystallization of garnet at the expense of hercynite+quartz according to the reaction (2) may also significantly increase the amount of Zn in the relic hercynite.

c) The potential existence of spinel with elevated of Fe_2TiO_4 component as a precursor of the assemblage hercynite+ilmenite+rutile, shown by common close association of hercynite and ilmenite (Fig. 2d), may indicate the presence of primary Ti-rich spinels a good indicator of UHT conditions (Sack & Ghiorso 1991; Sengupta et al. 1999); however, no relics of such a Ti-rich spinel were observed and the textural relations of hercynite+ilmenite are not convincing enough to provide evidence for the existence of Ti-rich spinel.

d) The concentrations of Zr in inclusions of rutile I enclosed in garnet cores and in prismatic sillimanite I is a novel method to determine T in UHT metamorphic rocks (Zack et al. 2004). The obtained data yielded T~840–910 °C in inclusions from garnet and slightly higher T~890–970 °C in inclusions enclosed in prismatic sillimanite I (see Fig. 4).

e) We applied geothermobarometry, disregarding the high degree of disequilibrium in kinzigite, to the garnet cores, where the enclosed minerals may be in equilibrium with the surrounding garnet. The garnet-ilmenite thermometer (Pownceby et al. 1991) yielded T=900±40 °C, the spinel-garnet geobarometer (Nichols et al. 1992) yielded P=0.68 GPa for temperature 900 °C, and 0.8 GPa for 950 °C. Disregarding the fact that formation of the assemblage ***A*** at T>~900 °C and P~0.5–0.7 GPa (or slightly higher) is supported by the lines of evidence discussed above; none of them is sufficiently convincing to confirm unequivocally the UHT metamorphic conditions in the Petrovice kinzigite.

The assemblage ***B*** garnet (X_{Mg}=0.30)+sillimanite replaced by cordierite II (X_{Mg}=0.68–0.69)±biotite is stable at T>~720 °C (Fig. 5) and high T~750 °C and P~0.5 GPa is also indicated by high X_{Mg} in cordierite II (e.g. Spear et al. 1999). The survival of hercynite during replacement of garnet by cordierite II in the stability field of hercynite+cordierite II suggests T>~800 °C for P~0.3 GPa and generally low pressure P<~0.5 GPa (Fig. 5) for the assemblage ***B***. The temperature T>~720–800 °C and P<~0.5 GPa is suggested for the assemblage ***B***.

The formation of Ti-rich biotite (up to 0.31 apfu Ti) in the assemblages ***C*** and ***D*** by the reactions including rutile and ilmenite (not specified in detail) also suggests a high temperature up to T~800 °C (cf. Sengupta et al. 1999). High Fe in biotite (X_{Mg}=0.47–0.44) relative to Mg-rich biotite from UHT metamorphic rocks (e.g. Carrington & Harley 1995; Sengupta et al. 1999) and the biotite obtained during experimental studies (e.g. Patiño Douce & Johnston 1991; Patiño Douce & McCarthy 1998; Kriegsmann & Hensen 1998; Sengupta et al. 1999) may reflect rather low pressure. The garnet-biotite thermometer calibrated according to Bhattacharya et al. (1992) yielded temperatures of 663–671 °C for the pressure 0.45 GPa. The abundance of K-feldspar in quartz-feldspar nests and absence of muscovite indicate P<~0.4 GPa during the late stage at T<~650 °C in the lower pressure side of the invariant point I (Fig. 5). Nevertheless, its position is controlled by the activity of H_2O and its lower activity shifts the invariant point I to a higher pressure (Holtz & Johannes 1996).

The sequence of the mineral assemblages in the garnet-sillimanite-cordierite kinzigite (***A*** to ***D***): cordierite I+

+ hercynite + rutile I + ilmenite + monazite + quartz → prismatic sillimanite I + garnet + ilmenite + rutile II → cordierite II ± biotite (± hercynite, ilmenite) → biotite + fibrolitic sillimanite II + + ilmenite, their textural relations (resorbed garnet), chemical composition (low Ca contents in garnet) and sequence of metamorphic reactions producing cordierite II (reactions 3–4) and consuming cordierite II (reactions 5–6) do not allow us to specify the *P-T* path in greater detail. However, some lines of evidence, such as low Ca contents in garnet and presence of the assemblage cordierite + hercynite, indicate low P<~0.5–0.7 GPa and high T>~800–950 °C. Consequently, an isobaric cooling path seems more likely relative to isothermal decompression (see Figs. 5, 6). High disequilibrium observed in the kinzigite as well as granophyric textures (Shelley 1993) developed locally in the leucosome indicates rapid cooling at relatively low water pressure, during the reactions producing the assemblages ***C*** and ***D***.

Garnet-orthopyroxene migmatites

The peak conditions of garnet-orthopyroxene migmatites could be estimated by comparison of the system published by Vielzeuf & Montel (1994). The authors estimated, for rocks of a similar composition (Qtz-Pl-Bt-bearing metagreywackes), that the Opx — in temperature range from 810 °C for the pressure 0.2 GPa, and 885 °C for 1 GPa. The Bt — out temperature from 860 °C for 0.2 GPa and 980 °C for 1 GPa. Garnet is stable by pressures higher than 0.5 GPa, whereas cordierite at lower pressure, spinel appears instead of garnet at temperatures higher than 850 °C. Therefore, the garnet-orthopyroxene-cordierite migmatites originated certainly at temperatures higher than 800 °C, and pressure higher than 0.5 GPa.

The skeletal form of garnet and high portion of unreacted biotite found in the biotite-plagioclase bands indicate that the temperature was not high enough to decompose the biotite completely, or the heat input was relatively short-lived, producing only a small amount of melt. The melt was just segregated, but not fully extracted from the parental gneiss. Kinzigite is, on the other hand, a restite after almost complete extraction of the melt. The absence of spinel and other minerals common as inclusions in garnet from kinzigite could be interpreted as evidence for relatively lower temperature origin of garnet-orthopyroxene-cordierite migmatites relative to kinzigite. The garnet-biotite thermometry yielded temperatures of 658–686 °C for the pressure 0.5 GPa. These values are almost identical with those, calculated from Grt-Bt pair in the kinzigite.

Potential heat source

The peak conditions of metamorphism at T up to ~800–950 °C and P~0.5–0.7 GPa estimated for the garnet-sillimanite-cordierite kinzigite from Petrovice and feasible isobaric cooling path (see discussion above) require an external heat source (cf. Spear 1993; Thompson 1999). The chemical U-Pb age (319 ± 24 Ma) of monazite closely associated with the assemblage ***A*** suggests the Variscan age of the HT to UHT metamorphism at T>~900 °C. In the region of the Petrovice kinzigite the following potential heat sources are discussed.

a) A large body of two-pyroxene ultrapotassic syenite to monzonite (Jihlava Pluton) located around the kinzigite body seems to be a dominant heat source in this region. Moreover, the radiometric age of the Jihlava Pluton's crystallization (U-Pb zircon, TIMS 335.2 ± 0.5 Ma, Kotková et al. 2003) is close to the chemical U-Pb age of the monazite 329.8 ± 9.5 Ma from the garnet-orthopyroxene-cordierite migmatites. The mineral assemblage in the garnet-orthopyroxene-cordierite migmatites from the exocontact of the Jihlava Pluton does not exhibit temperatures high enough to produce a high-grade melting and thus such a hyperaluminous restite–kinzigite with abundant sillimanite and hercynite. However, the retrograde (cooling) stage seems to be fairly similar to those from the kinzigite.

b) The gabbro-monzogabbro body occurring in close vicinity to the garnet-sillimanite-cordierite kinzigite with the calculated temperature of crystallization of monzogabbro at T ~ 1000–1100 °C (Leichmann et al. 2000) represents the possible heat source for the kinzigite. The U-Pb monazite age of the gabbro, 335.8 ± 6.9 (Leichmann & Švancara 2005) lies within the error of the kinzigite (319 ± 24 Ma) and Grt-Opx migmatite (329.8 ± 9.5 Ma) age estimation. The gabbroic intrusion may provide enough heat to produce high-degree melting of a metapelitic or metapsammitic protolith at temperatures ~900 °C (cf. e.g. Patiño Douce & Johnston 1991; Spear et al. 1999).

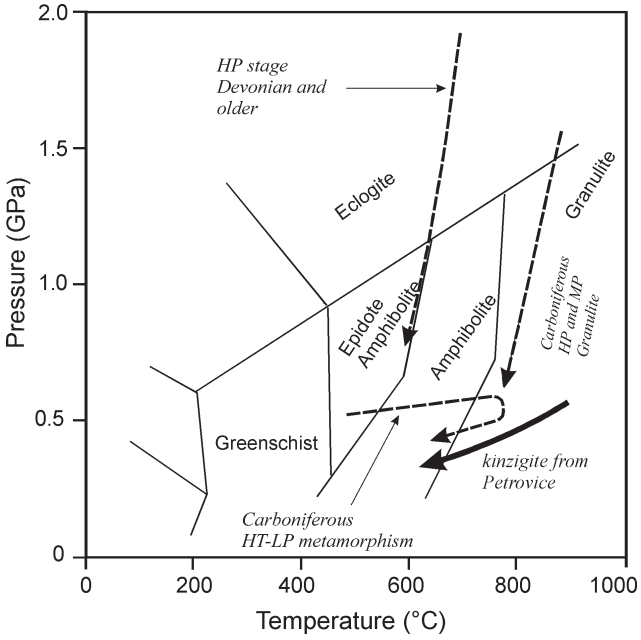

Fig. 7. Schematic *P-T* diagram modified after O'Brien (2000). Note that the *P-T* evolution of the garnet-sillimanite rock from Petrovice remarkably deviates from the three major Variscan *P-T* evolution paths known in the Bohemian Massif.

c) High heat flow to shallow crustal levels of 15 km (~0.5 GPa) subsequent to the Variscan collision (see Fig. 7) and crustal thickening is typical of the Moldanubian Zone (e.g. Montel et al. 1992; Kalt et al. 1999; Henk et al. 2000). Such a style of melting rather produced large-scale melting then small kinzigite body with the mineral assemblages showing a high degree of disequilibrium indicating rapid cooling.

In our scenario, the Jihlava Pluton may have served as a regional heat source with a modest heat contribution on a large scale. The intrusion of gabbro-monzogabbro represents a feasible heat source, which may have caused local overheating high enough to produce hyperaluminous kinzigite with the observed HT to UHT mineral assemblages. The close relation of the durbachite emplacement and tectonometamorphic evolution of the host rock is also pointed out by Verner et al. (2005).

Conclusions and summary

The garnet-sillimanite-cordierite kinzigite from Petrovice is characterized by hyperaluminous bulk chemical composition and mineral assemblages involving abundant garnet and prismatic sillimanite I with relics of cordierite I, hercynite, rutile I, ilmenite and quartz, and retrograde cordierite II, fibrolitic sillimanite II and Ti-rich biotite. The relic assemblages — cordierite + hercynite and hercynite + quartz may suggest peak metamorphism conditions at T ~ 900 °C and P ~ 0.5–0.7 GPa. We assume the kinzigite to be a restite, where a large portion of melt was extracted from the rock (see e.g. White & Powell 2002). Modest heat input from the Jihlava Pluton producing garnet-orthopyroxene migmatites supported by local but high heat input from a gabbro-monzogabbro body seems to be the important heat source. Nevertheless, the prograde history of the *P-T* path is uncertain, although the sequence of mineral reactions and garnet composition with low Ca suggest an isobaric cooling path for both kinzigites and Grt-Opx migmatites (see Figs. 5, 6). The chemical U-Pb age of monazite (319 ± 24 Ma) from the kinzigite related to assemblage *A* suggests a Variscan age of the HT to UHT metamorphism. The *P-T* evolution of the garnet-sillimanite rock from Petrovice remarkably deviates from three major Variscan *P-T* evolution paths known in the Bohemian Massif (Fig. 7) and interpretation of the potential tectonic scenario remains unclear. However, the cooling path resemble the cooling part of the Carboniferous HT-LP path (O'Brien 2000), but shifted to the higher temperature range.

Acknowledgments: We appreciate J. Kotková for her comments on the manuscript, M. Taylor for improving the language. This work was supported by the Grant Agency of the Czech Republic (Grant No. 205/03/0400) and the research project MSM. 0021622412. The authors thank P. Tropper and S. Vrána for their comments and suggestions.

References

Bűttner S. & Kruhl J.H. 1997: The evolution of a late-Variscan high-T/low-P region: the southeastern margin of the Bohemian massif. *Geol. Rdsch.* 86, 22–38.

Carrington D.P. & Harley S.L. 1995: Partial melting and phase relations in high-grade metapelites: an experimental petrogenetic grid in KFMASH system. *Contr. Mineral. Petrology* 120, 270–291.

Dallmeyer R.D., Franke W. & Weber K. (Eds.) 1995: Pre-Permian geology of the Central and Eastern Europe. *Springer*, Berlin, 1–213.

Dasgupta S., Sengupta P., Ehl J., Raith M. & Barchan S. 1995: Reaction textures in a suite of spinel granulites from the Eastern Ghats Belt, India: Evidence from polymetamorphism, a partial petrogenetic grid in the system KFMASH and the role of ZnO and Fe_2O_3. *J. Petrology* 36, 435–461.

Deibl I., Tropper P. & Mirwald P.W. 2003: The petrological evolution of high-grade metapelites from the Sauwald, southern Bohemian Massif. *Mitt. Österr. Miner. Gesell.* 148, 116–117.

Fiala F. & Losert J. 1976: Discovery of corundum, cordierite, garnet, sillimanite and tourmaline in herynite-rich rock at Chlum near Sepekov. *Čas. Mineral. Geol.* 21, 326 (in Czech).

Franke W. 2000: The mid-European segment of the Variscides: tectonostratigraphic units, terrane boundaries and plate tectonic evolution. In: Franke W., Haak V., Oncken O. & Tanner D. (Eds.): Orogenic processes: quantification and modelling in the Variscan Belt. *Geol. Soc. London, Spec. Publ.* 179, 35–61.

Henk A., von Blanckenburg F., Finger F., Schaltegger U. & Zulauf G. 2000: Syn-convergent high-temperature metamorphism and magmatism in the Variscides: a discussion of potential heat sources. In: Franke W., Haak V., Oncken O. & Tanner D. (Eds.): Orogenic processes: quantification and modelling in the Variscan Belt. *Geol. Soc. London, Spec. Publ.* 179, 387–400.

Holtz F. & Johannes W. 1996: Petrogenesis and experimental petrology of granitic rocks. *Springer*, Berlin, 1–333.

Kalt A., Berger A. & Blümel P. 1999: Metamorphic evolution of cordierite-bearing migmatites from the Bayerische Wald (Variscan Belt, Germany). *J. Petrology* 40, 601–627.

Kotková J., Schaltegger U. & Leichmann J. 2003: 338–335 Ma old intrusion in the E Bohemian massif — a relic of the orogen-wide durbachitic magmatism in European Variscides. *J. Czech. Geol. Soc.* 48, 1–2, 80–81.

Kretz R. 1983: Symbols for rock-forming minerals. *Amer. Mineralogy* 68, 277–279.

Kriegsman L.M. & Hensen B.J. 1998: Back reaction between restite and melt: Implications for geothermobarometry and pressure-temperature paths. *Geology* 26, 1111–1114.

Leichmann J. & Švancara J. 2005: Shoshonitic to ultrapotassic gabbros from the Jihlava pluton. *2. meeting of the Czech Geol. Soc.*, Slavonice, 151–153 (in Czech).

Leichmann J., Novák M., Zachovalová K. & Topa D. 2000: Ultrahigh temperature event in the Moldanubian Zone; its significance for the origin of durbachites. *Geolines* 10, 47.

Linner M. 1996: Metamorphism and partial melting of paragneisses of the Monotonous Group, SE Moldanubicum (Austria). *Mineral. Petrology* 58, 215–234.

Montel J.M., Marignac C., Barbey P. & Pichavant M. 1992: Thermobarometry and granite genesis: Hercynian low-P, high-T Velay anatectic dome (French Massif Central). *J. Metamorphic Geology* 10, 1–15.

Nekvasil H. 1992: Feldspar crystallization in felsic magmas: a review. *Trans. Roy. Soc. Edinburgh, Earth Sci.* 83, 399–407.

Nichols G.T., Berry R.F. & Green D.H. 1992: Internally consistent

gahnitic spinel-cordierite-garnet equilibria in the FMASHZn system: geothermobarometry and applications. *Contr. Mineral. Petrology* 111, 362–377.

Novák M. & Houzar S. 1996: The HT/LP metamorphism of dolomite marbles in the eastern part of the Moldanubicum; a manifestation of heat flow related to the Třebíč Durbachite Massif. *J. Czech. Geol. Soc.* 41, 139–146.

O'Brien P.J. 2000: The fundamental Variscan problem: high-temperature metamorphism in different depths and high-pressure metamorphism at different temperatures. In: Franke W., Haak V., Oncken O. & Tanner D. (Eds.): Orogenic processes: quantification and modelling in the Variscan Belt. *Geol. Soc. London, Spec. Publ.* 179, 369–386.

Patiño Douce A.E. & Johnston A.D. 1991: Phase equilibria and melt productivity in the pelitic system: implications for the origin of peraluminous granitoids and aluminous granulites. *Contr. Mineral. Petrology* 107, 202–218.

Patiño Douce A.E. & McCarthy T.C. 1998: Melting of crustal rocks during continental collision and subduction. In: Hacker B.R. & Liou J.G. (Eds.): When continents collide: geodynamics and geochemistry of ultrahigh-pressure rocks. *Kluwer Academic Publishers*, 27–55.

Petrakakis K. 1997: Evolution of Moldanubian rocks in Austria: review and synthesis. *J. Metamorphic Geology* 15, 203–222.

Pouchou J.L. & Pichoir F. 1985: "PAP" procedure for improved quantitative microanalysis. *Microbeam. Anal.* 20, 104–105.

Pownceby M.L., Wall V.J. & O'Neill H.St.C. 1991: An experimental study of effect of Ca upon garnet-ilmenite Fe-Mn exchange equilibria. *Amer. Mineralogist* 76, 1580–1588.

Sack R.O. & Ghiorso M.S. 1991: An internally consistent model for the thermodynamic properties of Fe-Mg-titano-magnetite-aluminate spinels. *Contr. Mineral. Petrology* 106, 474–505.

Sengupta P., Se J., Dasgupta S., Raith M., Bhui U.K. & Ehl J. 1999: Ultra-high temperature metamorphism of metapelitic granulites from Khondapalle, Eastern Ghats belt: Implications for the Indo-Antarctic correlation. *J. Petrology* 40, 1065–1087.

Shelley D. 1993: Igneous and metamorphic rocks under the microscope. *Chapman & Hall*, London, 1–445.

Shulters J.C. & Bohlen S.R. 1989: The stability of hercynite and hercynite-gahnite spinels in corundum- or quartz-bearing assemblages. *J. Petrology* 30, 1017–1031.

Spear F.S. 1993: Metamorphic phase equilibria and pressure-temperature-time paths. *Miner. Soc. Amer. Monograph*, Washington, 1–799.

Spear F.S., Kohn M.J. & Cheney J.T. 1999: P-T paths from anatectic pelites. *Contr. Mineral. Petrology* 134, 17–32.

Thompson A.B. 1999: Some time-space relationships for crustal melting and granitic intrusions at various depths. In: Castro A., Fernandez C. & Vigneresse L. (Eds.): Understanding granites: Integrating new and classical techniques. *Geol. Soc. London, Spec. Publ.* 168, 7–25.

Tonika J. 1970: Geology and petrology of the Jihlava massif. *Sbor. Geol. Věd, Ř. G.* 17, 105–119 (in Czech).

Verner K., Žák J., Holub F.V., Týcová P. & Nahodilová R. 2005: Textures and fabric of the durbachite plutons as an indicator of the tectonometamorphic evolution of the Moldanubicum (Czech Republic). *2. meeting of the Czech Geol. Soc.*, Slavonice, 101 (in Czech).

Vielzeuf D. & Holloway J.R. 1988: Experimental determination of the fluid-absent melting relations in the pelitic system: Consequences for crustal differentiation. *Contr. Mineral. Petrology* 98, 257–276.

Vielzeuf D. & Montel J.M. 1994: Partial melting of Al-metagreywackes. Part I. Fluid-absent experiments and phase relationships. *Contr. Mineral. Petrology* 117, 375–393.

Waters D.J. 1991: Hercynite-quartz granulite phase relations and implication for crustal processes. *Eur. J. Mineral.* 3, 567–586.

White R.W. & Powell R. 2002: Melt loss and the preservation of granulite facies mineral assemblages. *J. Metamorphic Geology* 20, 621–632.

Zack T., Moraes R. & Kronz A. 2004: Empirical calibration of a rutile thermometer and its application to UHT granulites. International workshop on petrogenesis of granulites and related rocks. *Moravian Museum*, Brno, 1–71.